Two-Site Binding of β-Cyclodextrin to the Alzheimer Aβ(1−40) Peptide Measured with Combined PFG-NMR Diffusion and Induced Chemical Shifts†

Jens Danielsson, Jüri Jarvet, Peter Damberg, and Astrid Gräslund*

Department of Biochemistry and Biophysics, The Arrhenius Laboratories for Natural Sciences, Stockholm University, SE-106 91 Stockholm, Sweden

Received December 16, 2003; Revised Manuscript Received March 5, 2004

ABSTRACT: The interactions of Alzheimer's amyloid β-peptide with cyclodextrins were studied by ^{1}H NMR: the translational diffusion coefficient of the peptide and chemical shift changes were studied by the presence of variable concentrations of cyclodextrins. For the full-length peptide, Aβ(1−40), the combined results of translational diffusion and chemical shift changes are consistent with a model where aromatic side chains interact with β-cyclodextrin with dissociation constants in the millimolar range. The diffusion data were consistent with two β-cyclodextrin molecules bound per peptide. The binding occurs at two sites, at F_{19} and/or F_{20} and at Y_{10}, with dissociation constants $K_d^F = 4.7$ mM and $K_d^Y = 6.6$ mM, respectively, in 10 mM sodium phosphate, pH 7.4 and 298 K. Shorter Alzheimer peptide fragments were studied to measure specific affinities for different binding sites. The N-terminal fragment Aβ(1−9) with a putative binding site at F_4 does not show measurable affinity for β-cyclodextrin. The fragment Aβ(12−28) has similar apparent affinity ($K_d = 3.8$ mM) to β-cyclodextrin as the full-length peptide Aβ(1−40). Here, the diffusion data suggests a one-to-one stoichiometry, and the binding site is F_{19} and/or F_{20}. Both diffusion results and chemical shift changes give the same affinity. A variant Aβ(12−28)$G_{19}G_{20}$ without phenylalanines does not bind to β-cyclodextrin. Other potential ligands, α-cyclodextrin, γ-cyclodextrin, nicotine, and nornicotine do not bind to the Aβ(12−28) fragment. This study shows that combined ^{1}H NMR diffusion and chemical shift changes may be used to quantitatively determine affinities and stoichiometries of weak interactions, using unlabeled ligands and hosts of comparable sizes.

The amyloid β-peptide (Aβ)[1] is the major component of the amyloid plaques found in the extracellular compartment in the brains of patients suffering from the Alzheimer's disease. The aggregation process giving rise to neurotoxic Aβ-peptide oligomers and consequently the formation of the neuritic plaques has been suggested to be an early pathological feature of Alzheimer's disease. This so-called amyloid hypothesis includes the self-aggregation of the Aβ-peptide into fibrils (*1*, *2*). The Aβ-peptide is a 39−42-residue peptide that is cleaved from the Alzheimer's precursor protein (APP) by the proteases β- and γ-secretase (*1*). In vitro, the cleaved peptide monomer is in a dominating random coil secondary structure in solution at room temperature and physiological pH (*3*). Toward lower temperatures, the secondary structure of the monomer changes gradually toward a left-handed 3_1 (PII) helix (*4*). The monomeric form is in equilibrium with aggregates of various sizes (*5*). The aggregation includes a conformational change of the peptide structure to β-sheet. There is experimental evidence that the soluble oligomers have toxic effects on neurons and synapses (*1*, *6*). Thus, peptide aggregation is an important feature in Alzheimer's disease as well as in other amyloid diseases.

Prevention of oligomerization and aggregation is one possible strategy of treatment of amyloid diseases. Examples of prevention are, for example, immunization where the antibodies reduce deposition of the aggregates, or metal chelation, where decreased binding of metal ions to the peptide may prevent aggregation (*1*). Another approach to this problem is the use of a ligand that binds to the monomeric state of the Aβ-peptide and prevents aggregation and structural change to β-sheet conformation, thus interfering with the process that leads to formation of fibrils and neuritic plaques.

The Aβ(1−40) peptide has two hydrophobic regions. The C-terminal region corresponds a part of the putative transmembrane segment of the APP, residues 29−40. The second hydrophobic region involves residues 17−21. This central region takes part in the in the aggregation process (*5*). The smallest fragment of the peptide known to form amyloid fibrils is the Aβ(16−22) fragment (*7*). Mutations in this central region alter the aggregation properties. Replacement of the phenylalanines at position 19 and 20 with glycines increases solubility and counteracts aggregation to a great extent (*8*).

It has been shown that the Aβ(12−28) fragment and the full-length peptide interact with β-cyclodextrin (*9*, *10*), and this interaction reduces fibril formation and neurotoxicity.

† This study was supported by grants from the Swedish Research Council.

* To whom correspondence should be addressed. Phone: +46 8 16 24 50. Fax: +46 8 15 55 97. E-mail: astrid@dbb.su.se.

[1] Abbreviations: NMR, nuclear magnetic resonance; Aβ, Alzheimer's β-peptide; APP, Alzheimer precursor protein; CD, circular dichroism; SPA, scintillation proximity assay; FCS, fluorescence correlation spectroscopy; PFG, pulsed field gradient; NOESY, nuclear Overhauser effect spectroscopy; TOCSY, total correlation spectroscopy; PFGSE, pulsed field gradient spin echo; PFGLED, pulsed field gradient longitudinal eddy-current delay; HPLC, high performance liquid chromatography.

10.1021/bi036254p CCC: $27.50
Published on Web 04/20/2004

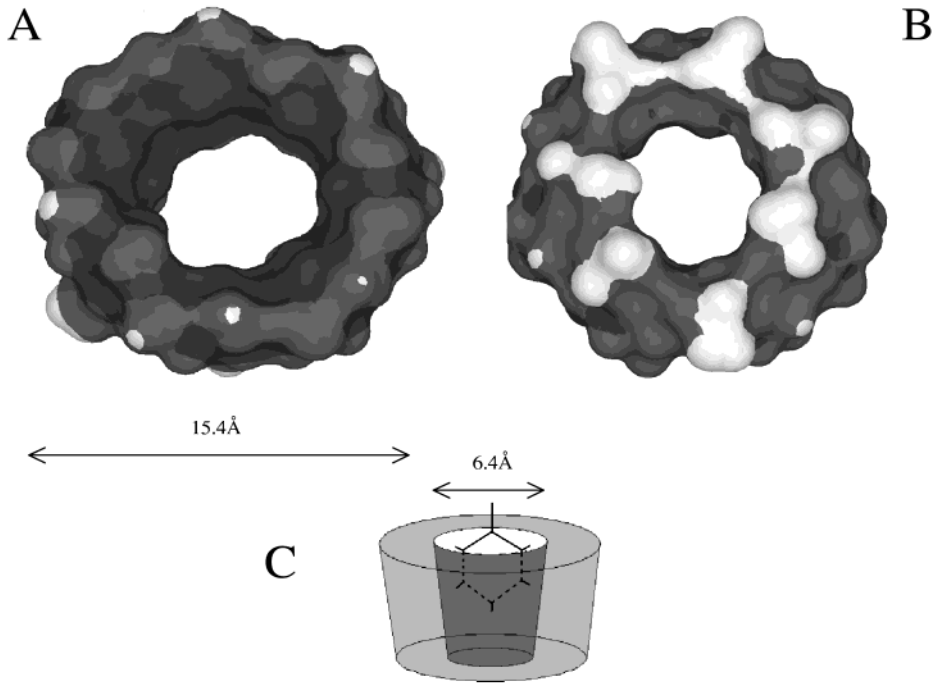

FIGURE 1: β-cyclodextrin and phenylalanine. The hydrophobic surface of β-cyclodextrin including the two sides of the sugar molecule with the wider opening (A) and the narrower opening (B) are shown. The dark areas are hydrophobic, and the bright areas are hydrophilic. The hydrophilic regions on the narrow opening side (B) are the primary hydroxyl groups. The size of an aromatic phenyl ring makes a good steric fit into the hydrophobic cavity of the β-cyclodextrin (C). Panel C shows a schematic picture of β-cyclodextrin from a side view with the aromatic ring in the cavity. The conical shape is exaggerated.

This interaction is considered to be hydrophobic in nature and has been suggested to involve the hydrophobic central part of the peptide and the hydrophobic cavity of the cyclodextrin. The interaction has previously been studied with circular dichroism (CD), nuclear magnetic resonance (NMR), mass-spectroscopy, and scintillation proximity assay (SPA) (*9*−*11*). The interacting residues are suggested to be F_{19} and F_{20}.

Cyclodextrins are a family of sugars consisting of cyclic oligosaccharides. They are torus shaped rings built up by different numbers of dextrin units. The three major types of cyclodextrins are the α-, β-, and γ-cyclodextrins in which the rings consist of six, seven, and eight sugar units, respectively. The different types of cyclodextrins have different characteristics mainly due to differences in size, but there are also some differences in chemical properties that cannot be explained solely with size (e.g., the solubility). α- and γ-cyclodextrin are more easily soluble in aqueous solution than β-cyclodextrin. The cyclodextrin molecules have some amphiphilic properties. The cavity of the torus is hydrophobic, while the rest is hydrophilic, making the cavities favorable places for hydrophobic interactions (Figure 1). In the ring, all primary hydroxyl groups, OH-6, are oriented to the side with the narrow opening, of the molecule, and the secondary hydroxyl groups, OH-2 and OH-3, are oriented to the other side. The primary hydroxyls are not able to move freely, but the secondary ones are. This means that the cavity toward which the secondary hydroxyl groups are facing is larger (i.e., it has a larger effective volume). The dimensions of the cavities are listed in Table 1. The smaller diameter corresponds to the narrower side. The differences in size of the hydrophobic cavity in the different cyclodextrins give possibilities of specificity in interaction (*12*).

Table 1: Cyclodextrins, Some Relevant Molecular Properties

	no of dextrins	mol.wt (Da)	diffusion[a] (10^{-10} m^2/s)	diameter of cavity[b,c] (Å)
α-cyclodextrin	6	972.9	2.65	5.3/4.7
β-cyclodextrin	7	1135.0	2.44	6.4/6.0
γ-cyclodextrin	8	1297.1	2.32	8.3/7.5

[a] Diffusion coefficient at 25 °C, dilute solution in D_2O, pH 7.4. [b] From ref *12*. [c] The two values correspond to the two sides of the cone-shaped molecule.

Earlier studies of the interaction between Aβ-peptide fragments and β-cyclodextrin show interaction between cyclodextrin and F_{19} or F_{20}. The inhibition of aggregation has been determined with SPA to a 50% inhibition at 5 mM concentration of β-cyclodextrin. Mass spectroscopy has shown that the stoichiometry of the reaction mainly is 1:1 (*9*).

Other substances have been suggested to interact with the Alzheimer peptide (e.g., melatonin and nicotine). Melatonin reduces toxicity and interacts with and inhibits β-sheet formation of the Aβ(1−40) (*13*). Nicotine has been suggested to reduce the formation of amyloid fibrils both by inhibiting formation and by disruption of preformed amyloid fibril (*14*). Interaction between Aβ-peptide and nicotine in the presence of SDS has been suggested to include binding of the pyrrolidine moieties of the nicotine to the histidines of the peptide (*15*). In vivo nicotine is metabolized, and one of the metabolites is nornicotine. The mechanism of reduced fibril formation by nicotine is not known, but it has been suggested that the nicotine metabolite nornicotine interacts with the Aβ-peptide and thereby reduces aggregation (*16*). Nornicotine has been suggested to covalently change the hydrophobic segment in the central region of the peptide, possibly by glycation of K_{16} (*16*).

The molecular interactions between Aβ-peptide and binding ligands can be studied by various methods, including light absorbance spectroscopy, circular dichroism spectroscopy, gradient centrifugation, surface plasmon resonance (SPR), and fluorescence correlation spectroscopy (FCS), all methods with their specific advantages and drawbacks. Using NMR diffusion measurements has the benefit of measuring in solution at conditions where the substrates are close to their native state. There is no need of labeling, neither with isotopes nor with probes. NMR measurements are also low energy measurements, and the dipole moments, which typically change in an electronically excited state, are not altered during the experiment. By using PFG NMR diffusion experiments, improved so that inhomogeneities of the magnetic field gradient are accounted for, high accuracy can be obtained in the measurements of the diffusion constants (*17*).

In this study, the interactions between Aβ-peptide, full-length as well as fragments of various sizes, and α-, β-, and γ-cyclodextrins were investigated by studies of NMR translational diffusion and ^{1}H chemical shift analysis. The interaction between the fragment Aβ(12−28) and nicotine and the nicotine metabolite nornicotine was studied as well.

MATERIALS AND METHODS

Theory and Methodology. Nuclear magnetic resonance (NMR) is a widely used tool to measure equilibrium constants (*18*). The constant is mostly determined by study of the chemical shift changes caused by the binding of a ligand to a host. This technique demands well-resolved resonances and well-defined chemical shift changes. Overlapping peaks require deconvolution, which reduces accuracy. Assuming a 1:1 complex, the dissociation constant K_d can be written in terms of total concentrations of the ligand and the actual populations of the host and the complex

$$K_d = \frac{(1 - p_{complex})([H]_0 - p_{complex}[L]_0)}{p_{complex}} \quad (1)$$

Here, the measured fraction of bound ligand, $p_{complex} = [C]/[L]_0$. [L], [H], and [C] are actual free ligand, free host, and complex concentrations, and the indices 0 indicate total concentration. The complex population has to be measured over a range of concentrations of ligand and/or host. One approach to measure the population with NMR is to use translational diffusion measurements. The measured diffusion coefficient is then the weighted mean value of the free and bound states of the ligand (*19*) when the ligand is in fast exchange between the bound and the free states on the time-scale of the diffusion experiment.

$$D_{obs} = (1 - p_{complex})D_{free} + p_{complex}D_{complex} \quad (2)$$

$$p_{complex} = \frac{D_{obs} - D_{free}}{D_{complex} - D_{free}} \quad (3)$$

The translational diffusion coefficients are denoted *D*. The two populations are in equilibrium, which can be slow on the chemical shift time scale (μs), resulting in two separate peaks corresponding to free and bound states, but fast on the translational diffusion time scale (ms), leading to an averaged observed diffusion coefficient (*20*). To ensure that no intermediate exchange phenomena interfere with the measurements of the diffusion coefficient, resonance peaks that do not show frequency shift upon titration should be used for measurements.

The diffusion coefficient is inversely proportional to the hydrodynamic radius of the particle as described in the Stokes−Einstein equation. The hydrodynamic radius is scaled with a power law of the mass. The exponent in the power law is a shape factor (*3*). Thus, when two substances, a ligand and a host, interact, there is a change in both the mass and in most cases, the shape. This makes the diffusion coefficient a sensitive observable when measuring interactions. From eq 3, it follows that if the diffusion coefficient of the complex is known, the population may be obtained in a single experiment. Then K_d is obtained from eq 1. This is however not always straightforward. The diffusion of the complex can be difficult to measure directly due to fast exchange, overlap in peaks, or small populations. If the host is substantially larger than the ligand, one can, however, with good accuracy approximate the diffusion coefficient of the complex with the diffusion coefficient of the host (*18*).

For a ligand with a size in the same order as the host, as in dimerization or protein−protein interactions or in the current study, one has to measure the diffusion coefficient over a range of ligand or host concentrations and fit the obtained data to eqs 1 and 2 assuming that a 1:1 binding model is valid. Eqs 1 and 2 can be combined to

$$D_{obs} = D_{free} + (D_{complex} - D_{free})\left[\frac{[L]_0 + [H]_0 + K_d}{2[L]_0} - \sqrt{\left(\frac{[L]_0 + [H]_0 + K_d}{2[L]_0}\right)^2 - \frac{[H]_0}{[L]_0}}\right] \quad (4)$$

If the condition that $D_{complex} \approx D_{host}$ is fulfilled, a one-parameter fit to eq 4 gives a smaller error than the single-experiment procedure described previously. A two-parameter fit is otherwise required with respect to $D_{complex}$ and K_d using a range of host concentrations.

If the interaction between the ligand and the host is weak and or when diffusion data with high accuracy is difficult to obtain (e.g. due to low sample concentration), the fitting of diffusion data to eq 4 with respect to both K_d and $D_{complex}$ can be unstable. Under such conditions, the diffusion coefficient of the complex has to be estimated, and a one-parameter fit has to be performed. Eq 4 is stable with respect to minor errors in $D_{complex}$ estimates. The relative error in K_d caused by an error in the estimated $D_{complex}$ is linear with the slope approximately 1 (data not shown).

The described model assumes a 1:1 stoichiometry. If the stoichiometry is of a different kind, then dissociation equation is written

$$K_d = \frac{[L]^m[H]^n}{[C]} \quad (5)$$

Here, the ligand to host stoichiometry is *m*:*n*, and [C] is the concentration of the *m*:*n* complex (*22*). Using a 1:1 stoichiometry model to evaluate a system with another stoichiometry gives errors in the calculated affinity. In the following treatment, a 1:1 stoichiometry is assumed unless

otherwise stated. It has been shown to be the most common stoichiometry in complexes including cyclodextrin (*12*).

When a complex is formed, the local environment of the observed spins change. Generally, this gives rise to changes in the local magnetic field and the chemical shift changes at the site involved in the binding. Observations of chemical shift changes upon complex formation may be used to further characterize the interactions in a complex, as for all NMR measurements the measured observable is the weighted mean of the states if the system is in fast exchange. Eqs 2 and 4 are valid for the chemical shift as well as for the diffusion coefficients. The chemical shift thus also gives information on the binding constant with the diffusion coefficient replaced by the corresponding chemical shifts and in addition indicates the site of binding.

NMR Methods. The spectrometers used for NMR experiments were a 600 MHz Varian Inova and a 500 MHz Bruker Avance equipped with a Bruker CryoProbe. All experiments were performed using spectrometers equipped with a *z*-axis gradient coil at 25 °C. NOESY experiments were performed to assign the resonances using standard procedures. TOCSY experiments were performed to study the chemical shift changes induced by interaction of the peptides with β-cyclodextrin.

NMR Diffusion Measurements. Diffusion measurements with NMR were performed with the pulsed field gradient spin−echo experiment (PFGSE) (*21*). The gradient coil does not generally create a constant gradient over the whole sample, and this produces a systematic error in the measurement. As previously described (*17*), this can be corrected for by the use of a distribution function for the gradient, a procedure that significantly increases the accuracy. The distribution function, assumed to be approximately linear, was calibrated using a substance with known diffusion coefficient, here a standard sample of 99.95% D_2O. The value of the HDO diffusion coefficient in D_2O at 25 °C used for the calibration is 1.90 10^{-10} m^2/s (*23*).

The Stejskal−Tanner spin−echo experiments to determine the diffusion coefficients were performed using a PFGLED (*24*) pulse sequence. A gradient prepulse was used to create a steady state to ensure that the second and third gradient pulses were equal (*25*, *26*). All experiments were performed using 16 (Bruker) or 30 (Varian) different linearly spaced strengths of gradients. The lengths of and delays between the gradient pulses were optimized depending on the studied substance and ranged between 4 and 5 ms and 65−100 ms, respectively. The number of scans ranged from 24 to 512 depending on the concentration of the measured peptide. All experiments were performed in pure D_2O, which has a higher viscosity than water. The viscosity of pure D_2O is a factor 1.23 higher at 25 °C (*23*, *27*, *28*). There is no need to account for the viscosity difference between D_2O and H_2O in the calculation because they do not change the binding constant. If the correct values of the diffusion coefficients in water are of interest, the presented values should be multiplied by 1.23.

Materials. The full-length Aβ(1−40) peptide was purchased from Neosystem, France and used without further purification. Some Aβ(1−40) was obtained as a gift from Oleg Antzutkin, who had made it by solid-phase synthesis and purified it by HPLC. The fragments Aβ(12−28), Aβ(1−9), l-diphenylalanine, and phenylalanine were purchased from Neosystem, France and used without further purification. The fragment KLVFFA was synthesized and purified by HPLC in our laboratory. The peptides were stored at −18 °C and thawed before used.

The experiments were performed with the peptides in 10 mM sodium phosphate buffer close to the physiological pH, ranging from 7.35 to 7.45. All pH values are corrected for isotope effects. The pH was adjusted using different fractions of NaH_2PO_4/Na_2HPO_4 and was measured on a standard pH-meter. The sample preparation was carried out at 5 °C. The quantities of solid materials were determined by weight, and the peptides were dissolved in prechilled pure (99.95%) D_2O. The low temperature during sample preparation was necessary to prevent peptide aggregation (*17*). The HDO resonance in the sample was used as an internal chemical shift reference. The reference value for HDO at 298.15 K is 4.753 ppm. All samples were prepared just prior to the experiments. The peptide concentration was 1 mM for all samples except for the full-length peptide, which was prepared in 100 μM concentration.

The cyclodextrins (α-, β-, and γ-cyclodextrin), nicotine, and nornicotine were purchased from Sigma Ltd., Germany. These substances were quantified by weight and dissolved in 20 mM sodium phosphate buffer. Once properly dissolved, the solution was chilled to 5 °C and was mixed in equal amounts with the peptide of choice, resulting in 0.5 mM peptide concentration (50 μM Aβ(1−40)) in a 10 mM buffer solution. The pH was measured prior to each NMR experiment.

RESULTS

Stability of the Binding Model. Using diffusion data to calculate the equilibrium constants of a weak interaction demands high accuracy on diffusion measurements. By the use of the modified Stejskal-Tanner experiment (*17*), one takes into account the spatial inhomogenities of the magnetic field gradient. This makes diffusion measurements more precise, and the typical error is less than 1%. These random errors in measured diffusion coefficients propagate into the calculation of K_d when fitting data to eq 4. To study the effect of errors in the diffusion measurements on the calculated equilibrium constant, numerical simulations were made. Real measured diffusion data were used, and an increasing random error was added to the data. The new data set was fitted to eq 4, and K_d and $D_{complex}$ were calculated. 5000 iterations were made at each error level ranging from 0 to 2% in increments of 0.01%, and the standard deviation of the fitted parameters was calculated. The propagation of error is approximately linear for small values in error in measured diffusion coefficients. An error less than 1% in diffusion coefficient corresponds to an error less than 35% in K_d and less than 2% in $D_{complex}$ (Supporting Information Figure 1S). It is clear that high accuracy is important when using diffusion data to calculate equilibrium constants.

High accuracy is also important to obtain high sensitivity in measuring the apparent dissociation constant for weak complexes. When studying a small peptide binding to a large host, the diffusion coefficient of the complex is very close to that of the free host. If the host is in large excess, dissociation constants of the order of 1 M can be measured. Weak interactions, on the other hand, give small changes in

Table 2: Results of Diffusion Measurements and Dissociation Constants Calculation for Interaction of Peptides with Cyclodextrins (Cd)[a]

peptide	Cd	D_{free} (10^{-10} m^2/s)	D_{bound} (10^{-10} m^2/s)	K_d (mM)[b]	error (mM)
phenylalanine	β	5.71	2.44	58.4	1.8
di-phenylalanine	β	4.39	2.15	10.1	2.0
KLVFFA	β	2.72	1.92	22.8	5.0
Aβ(1−9)	β	2.47	none[c]	none[c]	
Aβ(12−28)	β	1.76	1.66	3.84	1.2
Aβ(12−28)	α	1.76	none	none	
Aβ(12−28)	γ	1.76	none	none	
Aβ(12−28)$G_{20}G_{19}$	β	1.86	none	none	
Aβ(1−40)	β	1.25	1.20/1.17[d]	4.7/6.6[e]	2.0/3.1
				3.85[f]	2.0

[a] All values are viscosity corrected and measured in 10 mM sodium phosphate at pH 7.4 and 25 °C [b] Dissociation constant for F_{19} and/or F_{20}. [c] None denotes that no binding occurs. [d] Assuming one bound cyclodextrin or two bound cyclodextrins, respectively. [e] Dissociation constant for Y_{10}. [f] Assuming a one-to-one binding model.

the observed diffusion coefficients. These small changes are possible to measure if the diffusion measurements are precise and accurate. If the interactions are between substances of the same size, where one is in excess, dissociation constants of the order of 0.1 M can be measured with good precision.

1:1 Stoichiometry. When fitting the 1:1model, eq 4, to data obtained from an *m*:*n* stoichiometry, it is not easy to observe systematic errors in residuals from the fitting. However, the dynamic range of diffusion coefficient variation changes with different stoichiometry, where the change in diffusion coefficient is greater if more than one ligand binds to the peptide. Thus, the diffusion coefficient of the complex contains information on the stoichiometry, if the diffusion coefficient of the 1:1 complex differs from the diffusion coefficient of the 1:2 complex. This is the case, for instance, when the interacting species are of approximately the same size.

Diffusion Studies of the Aβ-Peptide, Full-Length and Fragments, and β-Cyclodextrin. The calibration of the gradient probes for the 600 MHz Varian and the 500 MHz Bruker were performed as previously described (*17*). Using these values, the diffusion experiments were performed using the PFGLED pulse sequence and fitting the obtained intensity decline as previously described (*17*). The residuals of data after fitting were studied to ensure that there was no systematic error arising from multicomponent diffusion. For each peptide, the diffusion coefficient was measured for the peptide alone, in the absence of a binding ligand (Table 2). The diffusion coefficients of all the five peptides were then measured with an increasing amount of β-cyclodextrin, starting at 1 mM to the solubility limit of 10 mM. The increasing amount of β-cyclodextrin affected the viscosity of the solution and thereby the measured diffusion coefficient. This was accounted for by measuring the HDO diffusion at each concentration and then correcting the measured value.

$$D_{corrected} = \frac{D_{HDO,neat}}{D_{HDO,measured}} D_{obs} \quad (6)$$

The viscosity dependence on β-cyclodextrin concentration, [β-Cd], is observed as the ratio $D_{HDO,neat}/D_{HDO,measured}$. This ratio is at a first approximation, and in this concentration interval, a linear function of [β-Cd]. With [β-Cd] in units of mM, $D_{corrected} = (1 + 0.00164[\beta\text{-Cd}])D_{obs}$. Without this correction, it would appear as if any substance added to the sample that affects the viscosity would exhibit a weak interaction, which is obviously not correct.

All diffusion measurements were made using integrated intensities of methyl proton region, and the measurements are all performed with uncertainty less than 1%. The error in the diffusion coefficient is specified as one standard deviation and thus has a confidence interval of 68%. The standard deviation is calculated from the deviation of data points from the fitted Stejskal−Tanner curve.

Figure 2 shows observed diffusion coefficients for Aβ(1−40) and Aβ(12−28) as functions of β-cyclodextrin concentration. The figures also include the fitted binding model functions, 1:2 and 1:1 peptide/β-cyclodextrin, respectively, for Aβ(1−40) (Figure 2A) and Aβ(12−28) (Figure 2B). Table 2 summarizes all measured diffusion coefficients and the dissociation constants evaluated from them using eq 4. The error limits indicated in the values of K_d were estimated by the deviation of the measured data from the binding curve. Monte Carlo simulations within the error limits of the diffusion coefficient gave more narrow error limits of K_d.

The full-length peptide and the Aβ(12−28) fragments bind β-cyclodextrin with a similar apparent affinity of $K_d = 3.8$ mM in 10 mM sodium phosphate, pH 7.4 and 25 °C. There are significant differences in peptide interactions with β-cyclodextrin (Table 2). The single phenylalanine binds very weakly with $K_d = 58.4$ mM. In this case, the interaction is so weak that the two parameter fit becomes unstable, and the diffusion coefficient of the complex had to be estimated. The phenylalanine molecule is significantly smaller than β-cyclodextrin, and its binding to the hydrophobic cavity would probably not change the diffusion of β-cyclodextrin to any large extent. The diffusion coefficient of the complex was then estimated to be the diffusion coefficient of β-cyclodextrin alone. The binding constants of the other fragments were calculated using the two-parameter fit. The full length Aβ(1−40) was studied at low concentration, 50 μM (Figure 2A). For this reason, the convergence radius of eq 4 becomes narrow, and the precision of the measured diffusion coefficients has to be high. The short fragment KLVFFA bound with $K_d = 22.6$ mM. l-Diphenylalanine was found to have a rather high affinity to β-cyclodextrin with $K_d = 10.1$ mM, higher than the KLVFFA fragment.

To study the importance of the two phenylalanine residues in the central hydrophobic region, the substituted Aβ(12−28)$G_{19}G_{20}$ was studied. This fragment does not bind to β-cyclodextrin to any measurable extent (Figure 2B). The original Aβ(12−28) peptide binds to β-cyclodextrin with $K_d = 3.8$ mM, the same K_d as for the full-length peptide (Figure 2B). The results with Aβ(12−28)$G_{19}G_{20}$ show that the phenylalanine residues 19 and 20 are crucial for the interaction. The fragment Aβ(1−9) was studied to determine the binding of β-cyclodextrin to the N-terminal phenylalanine F_4. No significant binding was observed for that phenylalanine. Figure 3 shows the populations of the different bound fragments as functions of β-cyclodextrin concentration.

The fragment Aβ(12−28) was found to bind to β-cyclodextrin with same apparent affinity as the full-length peptide (Table 2). The observed decrease in diffusion coefficient due

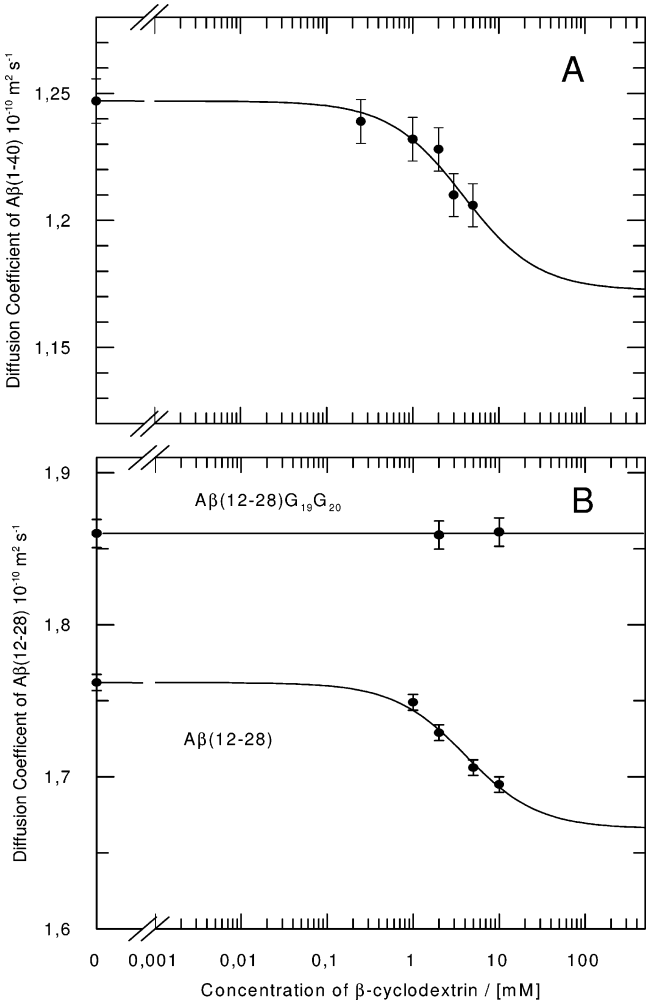

FIGURE 2: (A) Diffusion coefficients giving rise to a binding curve for the Aβ(1−40) full-length peptide interacting with β-cyclodextrin. The diffusion coefficients were measured with PFG NMR diffusion measurements and are all within 0.5% error. The measurements were performed at 16 different gradient strengths, equally distributed between 0 and 95% gradient strength. The peptide concentration was 50 μM, and the concentration of β-cyclodextrin ranges from 0 to 5 mM in 10 mM Na phosphate buffer (pH 7.4) and 25 °C. All data were viscosity corrected, as explained in the text. The two-parameter model was used to fit the data, and the apparent dissociation constant is K_d = 3.8mM. A two-site binding model gives two dissociation constants, one for phenylalanine and one for tyrosine, K_d^F = 4.7 mM and K_d^Y = 6.6 mM. (B) Diffusion coefficients giving rise to a binding curve for the Aβ(12−28) peptide interacting with β-cyclodextrin. The peptide concentration was 0.5 mM, and the β-cyclodextrin concentration was increased from 0 to 10 mM in buffer as described above. The apparent dissociation constant calculated is 3.8 mM. Diffusion results for the variant peptide Aβ(12−28)$G_{19}G_{20}$ are shown in the same figure. No binding occurs when the phenylalanines are absent. All data are viscosity corrected.

to binding is for the shorter fragment 5.8% and for the full-length peptide 8%. A simple spherical model shows that the relative change in diffusion coefficient of the fragment Aβ(12−28) would be twice the relative change of the diffusion coefficient of the full-length peptide when binding to one β-cyclodextrin. This relatively large change in diffusion coefficient for the complex suggests that more than one β-cyclodextrin binds to Aβ(1−40).

Chemical Shift Changes in the Aβ-Peptide, Full-Length and Fragments, Induced by β-Cyclodextrin. In the ^{1}H 1D NMR spectrum, the full-length peptide Aβ(1−40) showed

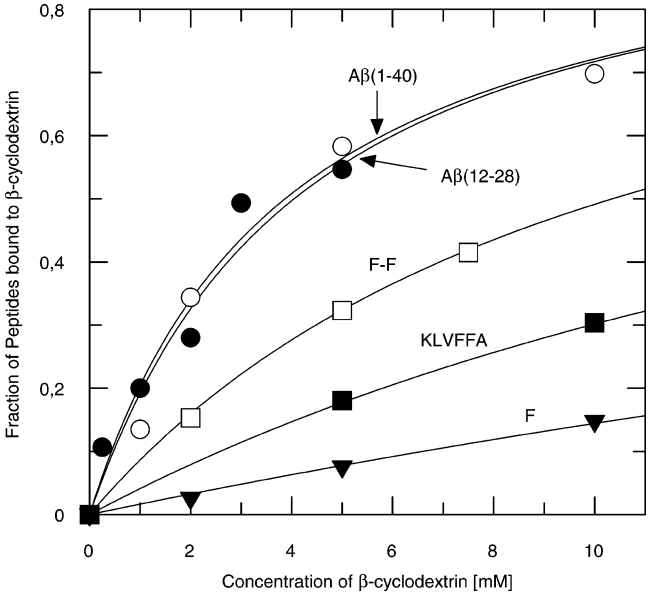

FIGURE 3: Populations of the studied peptides bound to β-cyclodextrin. From the observed D_{obs}, $D_{complex}$ was determined from eq 4; hence, the populations at each β-cyclodextrin concentration could be determined from eq 3. The curves shown are derived using the best-fitting dissociation constants K_d, listed in Table 2, in eq 1. The peptides are 0.5 mM phenylalanine (▼), 0.5 mM KLVFFA (■), 0.5 mM l-diphenylalanine (□), 50 μM full-length peptide Aβ(1−40) (●), and 0.5 mM Aβ(12−28) (○).

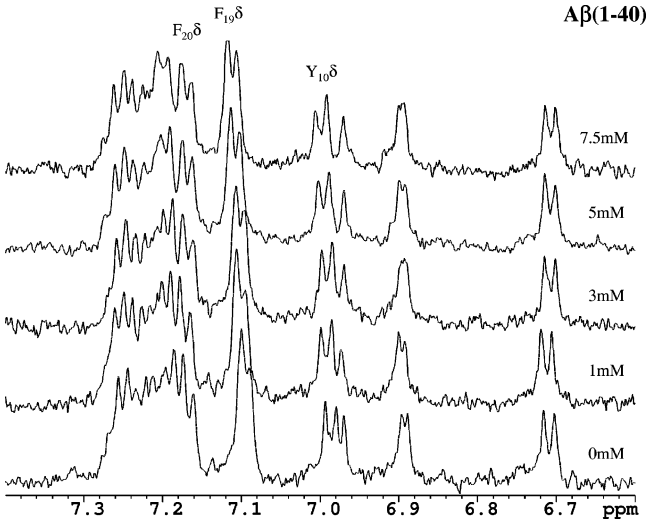

FIGURE 4: Resonances of the δ-protons of F_{19} and F_{20} in the full-length Aβ(1−40) peptide at increasing concentrations of β-cyclodextrin. The δ-proton resonance of F_{20} is unchanged with increasing concentration of β-cyclodextrin, in contrast to the corresponding resonances of F_{19} and Y_{10} that show chemical shift changes. The δ-proton resonance of F_4 overlaps partly with that of F_{19} and remains unchanged. The peptide concentration was 50 μM, and the β-cyclodextrin concentration ranged from 0 to 7.5 mM.

chemical shift changes of the δ-protons of F_{19} and also of the Y_{10} δ-protons, while no shift changes were observed for the δ-protons of F_{20}, when β-cyclodextrin was added (Figure 4 and Supporting Information Table 1S). Using the HDO resonance as an internal reference, chemical shifts could be determined with an accuracy of ±0.0005 ppm. For Aβ(12−28), we found that the δ-protons of F_{19} but not F_{20} exhibited significant shift changes when β-cyclodextrin was added (Supporting Information Figure 2S). At pH 7 and room temperature, the phenylalanine α-proton resonances overlap,

and TOCSY experiments were performed to resolve the spectra of Aβ(12−28). In the TOCSY spectra, the α-proton resonances of both F_{19} and F_{20} were shifted downfield with increasing amount of β-cyclodextrin (Supporting Information Table 1S). The resonances of the β-protons of the phenylalanines were resolved when no β-cyclodextrin is present but overlap more and more when the amount of β-cyclodextrin increases. The chemical shifts of the α-protons of the other residues remain unchanged in Aβ(12−28). The α-proton resonances of the phenylalanines (residues 4, 19, and 20) in Aβ(1−40) all overlap, and chemical shift changes are difficult to determine.

Quantitative information on ligand binding may also be determined from the chemical shift changes observed upon binding of the peptides to β-cyclodextrin. Using the α-proton chemical shift changes of F_{19} and F_{20} to calculate the dissociation constant gives $K_d = 2.7 \pm 0.5$ mM for Aβ(12−28), in agreement with diffusion data (Supporting Information Table 1S). Using the chemical shifts of the aromatic ring protons does not give results consistent with the diffusion results; for instance, when calculating the dissociation constant from the chemical shift of the phenylalanine δ-protons, the binding appears weaker, $K_d \approx 25$ mM.

Using the chemical shift changes of the δ-protons for Aβ(1−40), we found that also in this case the dissociation constants correspond to significantly weaker binding than calculated from the diffusion results. The intensity of the F_{19} δ-proton resonance shows that it overlaps with the δ-proton resonance of F_4. The line shape changes upon addition of β-cyclodextrin. Two overlapping peaks with slightly different splitting where one changes frequency while the other remains unchanged would reproduce this change in line shape, as shown in simulations (Supporting Information Figure 3S). The apparent chemical shift change is underestimated due to this kind of overlap, and consequently, the binding affinity is underestimated. The α-proton chemical shift of Y_{10} is, however, well-defined. Binding was calculated using the chemical shift changes of Y_{10} and was determined to be $K_d^{Y10} = 7.7 \pm 2.5$ mM. Using this value and the calculated dissociation constant of phenylalanine from the Aβ(12−28) fragment, a two-site model could be evaluated. The observed diffusion curve was simulated assuming an independent two-site binding. If one would use the one-site model (eq 4) to calculate the dissociation constant, this calculation gives $K_d^{\text{apparent}} = 3.34$ mM that agrees well with the experimental value 3.8 mM determined from diffusion measurements.

Using both experimental diffusion data and chemical shift changes and again assuming independent binding, one can calculate the dissociation constant of the phenylalanine binding site. From such a global fit with a two-site independent binding model, the calculated values of dissociation constants of the binding sites are $K_d^F = 4.7$ mM and $K_d^Y = 6.6$ mM. This gives the apparent dissociation constant $K_d^{\text{apparent}} = 3.8$ mM. This suggests that the peptide has two independent binding sites for β-cyclodextrin, a probably mutually exclusive site at F_{19} and/or F_{20}, and at Y_{10}.

Lack of Interaction with Other Cyclodextrins. The Aβ(12−28) fragment seems to be a good model system for the full-length peptide in studies of hydrophobic interactions. Thus, interactions with other hosts than β-cyclodextrin were studied with this fragment only. The diffusion coefficients of Aβ(12−28) in the presence of α- and γ-cyclodextrin were measured (Table 2). All data is viscosity corrected and shows that Aβ(12−28) does not bind to the smaller α- or the larger γ-cyclodextrin to any measurable extent under the present conditions. The experiments were performed with 10 mM α- or γ-cyclodextrin and 0.5 mM Aβ(12−28). In preliminary experiments, the smaller α-cyclodextrin did not bind to the full-length Alzheimer amyloid β-peptide either (data not shown). The viscosity corrected diffusion of the cyclodextrins alone was measured in control experiments and was found to be constant over the measured concentration range.

Lack of Interaction of Aβ(12−28) with Nicotine and Nornicotine. Nicotine and nornicotine have been suggested to interact with the Aβ-peptide and inhibit aggregation both by binding to the peptide and by disruption of already formed fibrils. No interactions of neither nicotine nor nornicotine with the fragment Aβ(12−28) could be observed by diffusion under conditions employed in the present study. By using diffusion measurements as described here, one should be able to detect any interaction with a dissociation constant of approximately 100 mM or less in the concentration range used for nicotine and nornicotine studies.

DISCUSSION

NMR translational diffusion measurements provide a powerful method to measure molecular interactions in a quantitative way. Both shape and size change due to binding and are reflected in the diffusion coefficient. Diffusion measurements have been used to determine equilibrium constants in recent studies (*18*−*20*, *22*). The present study shows that if the diffusion measurements are accurate and precise, weak interactions even between substrates of equal sizes can be measured with good precision. By taking into account the inhomogenities of the magnetic field gradient in standard NMR probes in the diffusion measurements, the accuracy of the diffusion measurements can be significantly improved (*17*). Thus, small changes in diffusion can be measured and weak interactions studied. The advantage of using NMR diffusion measurements is the fact that the substrates can be studied in solution, in a wide range of temperatures, without any added probes and without changing the excitation states and dipoles of the interacting molecules.

Binding of ligands to the Alzheimer peptide can be a strategy to affect the structural transition from random coil to β-sheet, which leads to aggregation. The interaction between Aβ-peptide and β-cyclodextrin has been shown previously (*9*−*11*). Here, we were able to characterize and quantitate the interaction between Aβ-peptide and β-cyclodextrin and to show that it has an apparent dissociation constant $K_d \cong 4$ mM at 25 °C, pH 7.4 in 10 mM phosphate buffer. The fact that the Aβ-fragment where F_{19} and F_{20} are replaced with glycines does not interact with β-cyclodextrin shows that these residues take part in the interaction. This is in good agreement with the suggestion (*10*) that it is the hydrophobic core of the peptide that is important for the interactions. Together with the diffusion studies, measurements of chemical shift changes induced by the interaction indicates that the full-length peptide interacts at two sites: the phenylalanines 19 and/or 20 and tyrosine 10. Here, it is

interesting to note that the interactions are not always manifested uniformly for all parts of a residue. The induced shifts of the resonances of the α-protons of F_{19} and F_{20} in Aβ(12−28) yield the same value of K_d as with diffusion measurements, whereas the aromatic resonances show induced shifts corresponding to a weaker binding of F_{19} and no binding of F_{20}. However, earlier NOE studies of β-cyclodextrin with Aβ(12−28) have shown cross-peaks to both phenylalanines (*9*). The full-length peptide has a third phenylalanine at position 4. The diffusion and induced chemical shift studies of Aβ(1−40) do not suggest binding of β-cyclodextrin to this phenylalanine to any measurable extent. This is supported by the fact that the N-terminal fragment Aβ(1−9) does not interact with β-cyclodextrin.

The peptide fragment Aβ(12−28) does not interact with the other two main groups of cyclodextrins, α- and γ-cyclodextrin. This suggests that a steric fit may be important. The cyclodextrins have hydrophobic cavities of different sizes depending on type. The aromatic rings of phenylalanine and tyrosine are approximately 2.5 Å in diameter between the carbons 3 and 5. Adding the hydrogens to this gives an effective diameter of approximately 5 Å (Figure 1). The hydrophobic cavity of β-cyclodextrin has a diameter of 6.5 Å, and this should make a good steric fit to the phenylalanine. α- and γ-cyclodextrins cavities seem to be too small or too large to give a good fit.

Chemical shift studies alone of these weak interactions give somewhat contradictory results. The aromatic resonances do not seem to follow directly the diffusion results. Using changes in α-proton chemical shifts seems to give better agreement with the diffusion results. The two-site model used assumes independent binding to Y_{10} and to F_{19} and/or F_{20}, meaning that binding at one site does not affect the affinity to bind to the other site. This is reasonable since the binding sites are separated by at least eight amino acids.

The weak binding of a single phenylalanine amino acid to β-cyclodextrin could reflect a weaker hydrophobicity of a single phenylalanine unit. With diphenylalanine, the binding increases 5-fold, and this may reflect an increase in hydrophobicity. Using calorimetry, the binding of phenylalanine to β-cyclodextrin has earlier been determined to be K_d = 55 mM (*29*), under similar conditions, in good agreement with our result K_d = 58 mM. The binding of the Aβ(12−28) fragment of the peptide and the full-length peptide are somewhat stronger than the dipeptide binding. The interacting phenylalanines, F_{19} and/or F_{20}, are surrounded by a hydrophobic milieu in the longer peptides, which may make the interacting region more hydrophobic than the dipeptide. Thus, there seems to be two factors that are crucial for the interaction: the nature of the residue itself and the hydrophobicity of the environment of the residue.

The short peptide corresponding to the central hydrophobic stretch KLVFFA does not bind as strongly as the full-length peptide or the 12−28 fragment. This short peptide is also more soluble (i.e., it is not as prone to aggregate as the longer fragments). Nicotine or nornicotine do no bind to the Aβ(12−28) under the present conditions.

Binding of β-cyclodextrin to the Aβ-peptide reduces the aggregation (*9*), but the binding is so weak that the reduction is not clinically important. Binding with a dissociation constant stronger than 100 μM should be necessary to reduce cell toxicity (*30*). The binding of the full-length peptide and the fragment Aβ(12−28) seems to be similar in strength. However, the experiments with the full-length peptide revealed yet another site of interaction, the Y_{10} residue, with only a slightly weaker affinity. This shows that β-cyclodextrin will target tyrosine as well as phenylalanine side chains in proteins and peptides. The two-site binding of β-cyclodextrin to Aβ(1−40) should make it possible to increase specificity by using both binding sites. To further increase affinity, derivatized forms of β-cyclodextrin can be used (*31*, *32*). This interaction might interfere with the oligomerization process of amyloid β-peptide.

ACKNOWLEDGMENT

We thank Oleg Antzutkin, who supplied part of the material of the full-length peptide.

SUPPORTING INFORMATION AVAILABLE

Chemical shift changes observed for F_{19} and F_{20} in Aβ(12−28) and for F_4, Y_{10}, F_{19}, and F_{20} in Aβ(1−40), when β-cyclodextrin was added; Monte Carlo simulation of the error propagation of the fitted parameters K_d and $D_{complex.}$; resonances of the δ-protons in phenylalanine 19 and 20 of the peptide fragment Aβ(12−28) at increasing β-cyclodextrin concentrations; and simulation of line shape changes for partly overlapping phenylalanine δ-proton resonances upon interaction with β-cyclodextrin. This material is available free of charge via the Internet at http://pubs.acs.org.

REFERENCES

1. Hardy, J., and Selkoe, D. J. (2002) The amyloid hypothesis of Alzheimer's disease: progress and problems on the road to therapeutics, *Science 297*, 353−356.
2. Kim, J. E., and Lee, M. (2003) Fullerene inhibits β-amyloid peptide aggregation, *Biochem. Biophys. Res. Commun. 303*, 576−579.
3. Danielsson, J., Jarvet, J., Damberg, P., and Gräslund, A. (2002) Translational diffusion measured by PFG-NMR on full length and fragments of the Alzheimer Aβ(1−40) peptide. Determination of hydrodynamic radii of random coil peptides of varying length, *Magn. Res. Chem. 40*, S89−S97.
4. Jarvet, J., Damberg, P., Danielsson, J., Johansson, I., Eriksson, L. E., and Gräslund, A. (2003) A left-handed 3_1 helical conformation in the Alzheimer Aβ(12−28) peptide, *FEBS Lett. 555*, 371−374.
5. Jarvet, J., Damberg, P., Bodell, K., Eriksson, L. G. E., and Gräslund, A. (2000) Reversible random coil to β-sheet transition and the early stage of aggregation of the Aβ(12−28) fragment from the Alzheimer peptide, *J. Am. Chem. Soc. 122*, 4261−4268.
6. Kuo, Y.-M., Webster, S., Emmerling, M. R., De Lima, N., and Roher, A. E. (1998) Irreversible dimerization/tetramization and posttranslational modifications inhibit proteolytic degradation of Aβ peptides of Alzheimer's disease, *Biochim. Biophys. Acta 1406*, 291−298.
7. Balbach, J. J., Ishii, Y., Antzutkin, O. N., Leapman, R. D., Rizzo, N. W., Dyda, F., Reed, J., and Tycko, R. (2000) Amyloid fibril formation by Aβ_{16-22}, a seven-residue fragment of the Alzheimer's β-amyloid peptide, and structural characterization by solid-state NMR, *Biochemistry 39*, 13748−13759.
8. Mansfield, S. L., Jayawickrama, D. A., Timmons, J. S., and Larive, C. K. (1998) Measurement of peptide aggregation with pulsed-field gradient nuclear magnetic resonance spectroscopy, *Biochim. Biophys. Acta 1382*, 257−265.
9. Camilleri, P., Haskins, N. J., and Howlett, D. R. (1994) β-Cyclodextrin interacts with the Alzheimer amyloid β-A4 peptide, *FEBS Lett. 341*, 256−258.
10. Qin, X. R., Abe, H., and Nakanishi, H. (2002) NMR and CD studies on the interaction of Alzheimer β-amyloid peptide (12−28) with β-cyclodextrin, *Biochem. Biophys. Res. Commun. 297*, 1011−1015.

11. Amersham Pharmacia Biotech (1999) A Scintillation Proximity Assay to Measure Aggregation of β-Amyloid 1−40, *Proximity News 45*, 1−4.
12. Szejtli, J. (1998) Introduction and General Overview of Cyclodextrin Chemistry, *Chem. Rev. 98*, 1743−1754.
13. Skribanek, Z., Balászpiri, L., and Mák, M. (2001) Interaction between synthetic amyloid-β-peptide (1−40) and its aggregation inhibitors studied by electrospray ionization mass spectrometry, *J. Mass Spectrom. 36*, 1226−1229.
14. Ono, K., Hasegawa, K., Yamada, M., and Naiki, H. (2002) Nicotine breaks down preformed Alzheimer's β-amyloid fibrils in vitro, *Biol. Psychiatry 52*, 880−886.
15. Salomon, A. R., Marcinowski, K. J., Friedland, R. P., and Zagorski, M. G. (1996) Nicotine inhibits amyloid formation by the β-peptide, *Biochemistry 35*, 13568−13578.
16. Dickerson, T. J., and Janda, K. D. (2003) Glycation of the amyloid β-protein by a nicotine metabolite: a fortuitous chemical dynamic between smoking and Alzheimer's disease, *Proc. Natl. Acad. Sci. U.S.A. 100*, 8182−8187.
17. Damberg, P., Jarvet, J., and Gräslund, A. (2001) Accurate measurement of translational diffusion coefficients: a practical method to account for nonlinear gradients, *J. Magn. Reson. 148*, 343−348.
18. Cameron, K. S., and Fielding, L. (2001) NMR diffusion spectroscopy as a measure of host−guest complex association constants and as a probe of complex size, *J. Org. Chem. 66*, 6891−6895.
19. Derrick, T. S., Lucas, L. H., Dimicoli, J.-L., and Larive, C. K. (2002) ^{19}F diffusion NMR analysis of enzyme−inhibitor binding, *Magn. Res. Chem. 40*, S98−S105.
20. Jayawickrama, D. A., and Larive, C. K. (1999) Analysis of the (trimethylsilyl)propionic acid-β(12−28) peptide binding equilibrium with NMR spectroscopy, *Anal. Chem. 71*, 2117−2122.
21. Stejskal, E. O., and Tanner, J. E. (1965) Spin Diffusion Measurements: Spin Echoes in the Presence of a Time-Dependent Field Gradient, *J. Chem. Phys. 42*, 288−292.
22. Wimmer, R., Aachmann, F. L., Larsen, K. L., and Petersen, S. B. (2002) NMR diffusion as a novel tool for measuring the association constant between cyclodextrin and guest molecules, *Carbohydr. Res. 337*, 841−849.
23. Longsworth, L. G. (1960) The Mutual Diffusion of Light and Heavy Water, *J. Phys. Chem. 64*, 1914−1917.
24. Gibbs, S. J., and Johnson, C. S. (1991) A PFG NMR experiment for accurate diffusion and flow studies in the presence of eddy currents, *J. Magn. Reson. 93*, 395−402.
25. von Meerwall, E., and Kamat, M. (1989) Effect of Residual Field Gradients on Pulsed-Gradient NMR Diffusion Measurements, *J. Magn. Reson. 83*, 309−323.
26. Yao, S., Howlett, G. J., and Norton, R. S. (2000) Peptide self-association in aqueous trifluoroethanol monitored by pulsed field gradient NMR diffusion measurements, *J. Biomol. NMR 16*, 109−119.
27. Cho, C. H., Urquidi, J., Singh, S., and Robinson, G. W. (1999) Thermal offset viscosities of liquid H_2O, D_2O, and T_2O, *J. Phys. Chem. 103*, 1991−1994.
28. Mills, R. (1973) Self-Diffusion in Normal and Heavy Water in the Range 1−45°, *J. Phys. Chem. 77*, 685−688.
29. Castronuovo, G., Elia, V., Fessas, D., Giordano, A., and Velleca, F. (1995) Thermodynamics of the interaction of cyclodextrins with aromatic and α, ω-amino acids in aqueous-solutions—a calorimetric study at 25 °C, *Carbohydr. Res. 272*, 31−39.
30. Cairo, C. W., Strzelec, A., Murphy, R. M., and Kiessling, L. L. (2002) Affinity-based inhibition of β-amyloid toxicity, *Biochemistry 41*, 8620−8629.
31. Yu, J., Bakhos, L., Chang, L., Holterman, M. J., Klein, W. L., and Venton, D. L. (2002) Per-6-substituted β-cyclodextrin libraries inhibit formation of β-amyloid-peptide (Aβ)-derived, soluble oligomers, *J. Mol. Neurosci. 19*, 51−55.
32. Chang, L., Bakhos, L., Wang, Z., Venton, D. L., and Klein, W. L. (2003) Femtomole immunodetection of synthetic and endogenous amyloid-β oligomers and its application to Alzheimer's disease drug candidate screening, *J. Mol. Neurosci. 20*, 305−313.

BI036254P